PHYSICAL REVIEW B **72**, 115426 (2005)

Pull-in characteristics of electromechanical switches in the presence of Casimir forces: Influence of self-affine surface roughness

G. Palasantzas* and J. Th. M. De Hosson
Department of Applied Physics, Materials Science Center and the Netherlands Institute for Metals Research, University of Groningen, Nijneborgh 4, 9747 AG Groningen, The Netherlands

(Received 12 May 2005; revised manuscript received 11 July 2005; published 22 September 2005)

In this work we explore the influence of self-affine roughness on the pull-in parameters for switches used in micro/nanoelectromechanical devices in the presence of the Casimir force. The pull-in parameters are described, respectively, by the ratios of the Casimir and electrostatic forces with respect to that of an elastic restoring force. It is shown that the roughness exponent H, which for self-affine roughness characterizes the degree of surface irregularity at short length scales, has significant influence on the Casimir force and consequently on the pull-in parameters. Indeed, significant changes of the ratio of the Casimir to restoring force take place for roughness exponents $H<0.5$, while larger exponents (>0.5) have an effect that saturates rather fast especially for values close to that of a smooth hill-valley topography ($H\sim 1$). For the ratio of the electrostatic to restoring force, the influence of the roughness exponent H is less prominent for relatively large normalized plate separations (with respect to the initial separation in the absence of any forces). In any case, the largest influence of the roughness exponent H on the ratio of the Casimir to restoring force takes place for relatively weak electrostatic forces.

DOI: 10.1103/PhysRevB.72.115426 PACS number(s): 68.55.−a, 68.60.Bs, 87.50.Rr, 85.70.Kh

I. INTRODUCTION

A fundamental building block in the design of micro/nanoelectromechanical (MEMS/NEMS) applications such as nanotweezers, nanoscale actuators, etc., are micoswitches.[1,2] The latter systems possess an inherent instability that is known as the pull-in phenomenon. Typically a switch is constructed from two conducting electrodes where one is usually fixed and the other one is able to move in a manner that it is suspended by using a mechanical spring. By applying a voltage difference between the two electrodes, the upper movable electrode displaces towards the ground electrode because of the electrostatic force. At a certain voltage, the moving electrode becomes unstable and collapses or pulls-in to the ground plane. The voltage and gap distance of the switches at this state are the so-called pull-in voltage and the pull-in gap, respectively (pull-in parameters).

Analytical expressions of the pull-in parameters of MEM switches are given in Ref. 3. A two-degrees of freedom pull-in model is presented in Ref. 4 for a direct calculation of the electrostatic actuators. The effect of residual charges (located in dielectric coating layers) on the pull-in parameters of electrostatic actuators has been studied in Ref. 5. Residual stress and fringing-field effect have a great influence on the behavior of rf switches, and even originate the failure of the devices.[6]. The pull-in phenomenon takes place in a variety of micromachined devices that require bistability for their operation as for example the electrical rf switches,[7] and some other micro-optoelectromechanical systems (MOEMS) devices.[8]. The bifurcation analysis for an electrostatic microactuator was addressed in Refs. 9 and 10. The pull-in voltage in the presence of van der Waals forces was studied in Ref. 11, while omitting its influence on the pull-in gap. However, in Ref. 12 it was considered the effect of van der Waals force on the pull-in gap and gave an analytical expression of the pull-in gap and pull-in voltage based on a more general model.

The dynamical behavior for nanoscale electrostatic actuators was studied by considering the effect of the van der Waals force in Ref. 13. The Casimir effect on the pull-in gap and pull-in voltage of NEMS switches was also studied in Ref. 10. An approximate analytical expression of the pull-in gap with the Casimir force was presented in terms of perturbation theory.[14] Moreover, the influence of the Casimir force on the nonlinear behavior of nanoscale electrostatic actuators was studied recently in detail.[15] A one-degree of freedom mass-spring model was adopted and the bifurcation properties of the actuators were obtained.[15]

The Casimir effect in its simplest form describes the attraction between two parallel conducting plates separated by a distance d where the attractive force is proportional to the surface area of the parallel plates.[16] This is a prediction of quantum electrodynamics, which arise from the perturbation of zero point vacuum fluctuations of the electromagnetic field by the conducting plates. The fundamental nature of the Casimir effect and its implications, e.g., on surface forces,[17] particle physics,[18] cosmology,[19] etc., has lead to wide theoretical work.[20–24] Up to now the previous studies did not consider the influence of plate roughness through the Casimir effect on the pull-in parameters foe NEMS/MEMS. Indeed, in many cases the roughness of deposited metal layers is termed as self-affine.[25] Any investigation for the roughness influence for the case of random self-affine rough plates is still missing, and that will be the topic of the present paper. In this case, besides of the rms roughness amplitude w and the lateral correlation length ξ, the short wavelength roughness also plays a critical role. The latter is characterized by a roughness exponent $H(0<H<1)$, which is a measure of the degree of surface irregularity.[25]

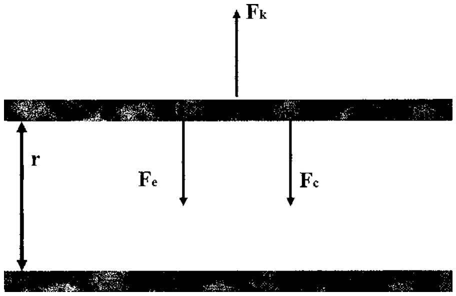

FIG. 1. Schematic of the device geometry under consideration in the present work.

II. SYSTEM THEORY

We consider a parallel plate configuration as shown in Fig. 1. The electrostatic force (neglecting fringing fields) and the Casimir force pull the two parallel plates together, while an elastic restoring force (with mass-spring form) opposes this movement. The initial plate distance is considered to be d and the average flat plate surface area to be A_{flat}. We denote also by k as the spring constant of the beam or plate, V as the voltage across the plates, and ε_0 as the permittivity of vacuum. The restoring force is assumed to take the standard mass-spring form[15]

$$F_k = -k(d-r). \tag{1}$$

The spring constant k depends on the cross-section shape as well as on the boundary conditions. The electrostatic force (ignoring fringes effects) is given by[15]

$$F_e \cong \frac{\varepsilon_0 A_r}{2}\frac{V^2}{r^2} \tag{2}$$

with A_r as the rough plate surface area, where it is assumed (for simplicity reasons) that for both plates in Fig. 1 we have the same roughness. The Casimir force in the limit of flat plate surfaces A_f is given by[16,26]

$$F_{cf} = -\frac{dE_{cf}}{dr} = \frac{\pi^2 c}{240 r^4}A_f \quad \text{since} \quad E_{cf} = -\frac{\pi^2 c}{720 r^3}A_f. \tag{3}$$

For rough metal plates assuming single valued roughness fluctuations $h(R)$ of the in-plane position $R=(x,y)$ (and ignoring roughness crosscorrelations) we have for plate separations r[26]

$$E_{cr} \cong E_{cf} + \frac{1}{2}\left(\frac{\partial^2 E_{cf}}{\partial r^2}\right)\sum_{m=1}^{2}\int \frac{d^2q}{(2\pi)^2}P_m(q)\langle|h_m(q)|^2\rangle \tag{4}$$

with $\langle|h_{mm}(q)|^2\rangle$ as the roughness spectra of both surfaces ($\langle h_m\rangle=0$). The function $P_m(q)$ is given by[27]

$$P_m(q) = [G_{TM}(qr/2\pi) + G_{TE}(qr/2\pi)]/[G_{TM}(0) + G_{TE}(0)]. \tag{5}$$

The functions G_{TM} and G_{TE} correspond to the contributions of TM and TE modes.[27] In the limit of large plate distances so that $d \gg \lambda_p$ with λ_p as the surface plasmon wavelength (e.g., for Al $\lambda_p \approx 100$ nm), we have $P_m(q)=C_0 qr$ with $C_0 = \frac{1}{3}$ and $qr > 1$.[26] Upon substitution of Eq. (5) into Eq. (4) we obtain

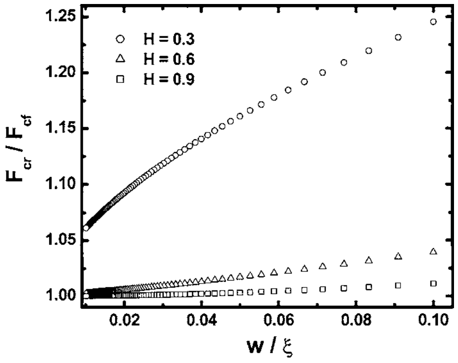

FIG. 2. The Casimir force vs ratio w/ξ for various roughness exponents H and fixed roughness amplitude $w=10$ nm.

$$E_{cr} \cong E_{cf} + \frac{1}{2}\left(\frac{\partial^2 E_{cf}}{\partial r^2}\right)(C_0 r)\tilde{C}_r,$$
$$\tilde{C}_r = \sum_{m=1}^{2}\int_{Q_d}^{Q_c} q\langle|h_m(q)|^2\rangle\frac{d^2q}{(2\pi)^2}, \tag{6}$$

where the Casimir force is given in this case by $F_{cr} = -dE_{cr}/dr$, $Q_d=2\pi/d$, and $Q_c=\pi/a_0$ where a_0 is of the order of atomic dimensions. Substitution of Eq. (6) and term rearrangement yields

$$F_{cr} \cong F_{cf}\left(1 + \frac{2C_r}{3r}\right), \tag{7}$$

where the factor 2 in front of C_r appears because we assume having the same roughness on both sides of the plates so that $C_r=2C_r$. Furthermore, the electrostatic force and the Casimir force are attractive, and the restoring force is repulsive. Therefore, according to Newton second law, we obtain the equation of motion of this model as

$$m\frac{d^2r}{dt^2} = |F_k| - |F_e + F_{cr}|, \tag{8}$$

where m is the mass of the moving plate (or beam).

III. ROUGHNESS MODEL

In order to solve Eq. (8) and to perform a stability analysis of the system, knowledge of the roughness spectra $\langle|h_m(q)|^2\rangle$ is necessary. Indeed, a wide variety of surfaces and interfaces appearing in various physical systems (i.e., films grown under nonequilibrium conditions) possess a so-called self-affine roughness.[25] In this case, the roughness spectrum $\langle|h(q)|^2\rangle$ shows the power law scaling[25]

$$\langle|h(q)|^2\rangle \propto q^{-2-2H} \text{ if } q\xi \gg 1 \text{ and } \langle|h(q)|^2\rangle \propto \text{const if } q\xi \ll 1. \tag{9}$$

This scaling is satisfied by the analytic model[28]

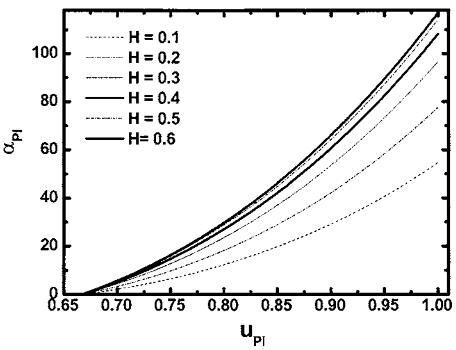

FIG. 3. Parameter α_{PI} vs u_{PI} for various roughness exponents H, $d=100$ nm, $\xi=200$ nm, and $w=10$ nm.

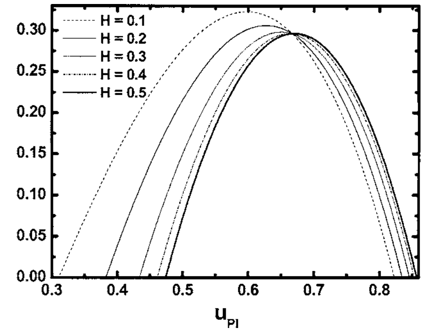

FIG. 4. Parameter β_{PI} vs u_{PI} for various roughness exponents H, $d=100$ nm, $\xi=200$ nm, and $w=10$ nm.

$$\langle |h(q)|^2\rangle = [2\pi w^2\xi^2/(1+aq^2\xi^2)^{1+H}] \tag{10}$$

with $a=\frac{1}{2}H[1-(1+aQ_c{}^2\xi^2)^{-H}](0<H<1)$, and $a=\frac{1}{2}\ln(1+aQ_c{}^2\xi^2)(H=0)$[28] $Q_c=\pi/a_0$ with a_0 of the order of atomic dimensions. Note that small values of H (about equal to 0) characterize extremely jagged or irregular surfaces; while large values H (about equal to 1) refer to surfaces with smooth hills and valleys.[25] The choice of the experimental parameters (w, ξ, and H) used in this study is based on real experimental films grown under nonequilibrium conditions as it is well documented in Ref. 25. Our particular model for the roughness spectrum is used for illustration purposes only, while in real NEMS/MEMS the measurement of the correction function should be used to derive the proper real correlation data.[25,28] In addition, for other roughness models see also Ref. 29.

Figure 2 shows calculations of the Casimir force from Eqs. (7) and (9). It is clearly seen that the roughness exponent H has a prominent effect on the Casimir energy with respect to the long wavelength roughness ratio w/ξ, i.e., for fixed roughness amplitude w. Since $\langle |h(q)|^2\rangle \propto w^2$, the Casimir force F_{cr} will have a simple dependence on w or $F_{cr} \propto w^2$, while any more complex dependence will arise from the parameters H and ξ. Therefore, proper surface roughness measurements are necessary to characterize the morphology at all relevant roughness wavelengths in order to gauge its influence on the Casimir force. We should point out that the perturbative calculations of the Casimir force always lead to roughness correction that is larger than the result obtained within the proximity force approximation (PFA).[27,30] Moreover, in the present work we consider our calculations for the case of perfectly reflecting mirrors assuming plate separations $r>\lambda_p$,[27] while for shorter distances the effect of finite conductivity should taken into account. The more general case for arbitrary plasma wavelength was investigated recently for Gaussian roughness correlation function $\langle |h(q)|^2\rangle \propto w^2 e^{-q^2\xi^2/4}$ and metallic plates described by the plasma model.[30]

IV. STABILITY ANALYSIS AND DISCUSSION

Upon change of variables so that $u=r/d$, $M=m/kT^2$, $\tau=t/T$ with T as a characteristic time, $\alpha=\pi^2\ A_f/kd^5$ (i.e., the ratio between the Casimir and restoring forces), $\beta=\varepsilon_0 A_r V^2/kd^3$ (i.e., the ratio between the electrostatic and restoring forces), Eq. (8) takes the form

$$M\frac{d^2u}{d\tau^2} = f(\alpha,\beta,u) = 1-u-\frac{\beta}{2u^2}-\frac{\alpha}{240u^4}\left(1+\frac{2C_r}{3du}\right). \tag{11}$$

Note that the parameter β in Eq. (11) contains the rough surface area A_r that was defined before for the electrostatic force in Eq. (2). According to the definition of these parameters, physically meaningful solutions exist in the region $0<u<1$. In order to obtain equilibrium we need to have $f(\alpha,\beta,u)=0$ where stability is obtained if and only if $df/du<0$. At the critical condition $df/du=0$ we obtain

$$\frac{\alpha}{60u}+\frac{\alpha}{72u^2}\frac{C_r}{d}+\beta u-u^4=0. \tag{12}$$

Solving $f(\alpha,\beta,u)=0$ and Eq. (12) we obtain the pull-in parameters β_{PI} ($\propto V_{PI}{}^2$ with V_{PI} the pull-in voltage), α_{PI}, and the pull-in gap u_{PI} so that (see also the Appendix)

$$\beta_{PI}=u_{PI}^3-\frac{\alpha_{PI}}{60u_{PI}^2}\left(1+\frac{5}{6}\frac{C_r}{u_{PI}d}\right),$$
$$\alpha_{PI}=(-240u_{PI}{}^4+360u_{PI}{}^5)\left(1+\frac{C_r}{d}\frac{1}{u_{PI}}\right)^{-1}. \tag{13}$$

Furthermore, the solution of Eqs. (13) yields for the pull-in voltage the expression as a function of the pull-in gap

$$V_{PI}=\sqrt{\frac{kd^3}{\varepsilon_0 A_r}\left[u_{PI}^3-\frac{\alpha_{PI}}{60u_{PI}^2}\left(1+\frac{5}{6}\frac{C_r}{u_{PI}d}\right)\right]}, \tag{14}$$

where further consideration of the roughness influence on the rough surface area A_{rou} can be given if we assume a Gaussian height-height distribution where in that case we have[31]

$$A_r=A_{flat}\int_0^{+\infty} e^{-y}(1+\rho_{rms}{}^2 y)^{1/2}dy,$$
$$\rho_{rms}=\left[\int_0^{Q_c} q^2\langle |h(q)|^2\rangle\frac{d^2q}{(2\pi)^2}\right]^{1/2}, \tag{15}$$

where $\rho_{rms}=[\langle|\nabla h|^2\rangle]^{1/2}$ is the rms local surface slope.[32]

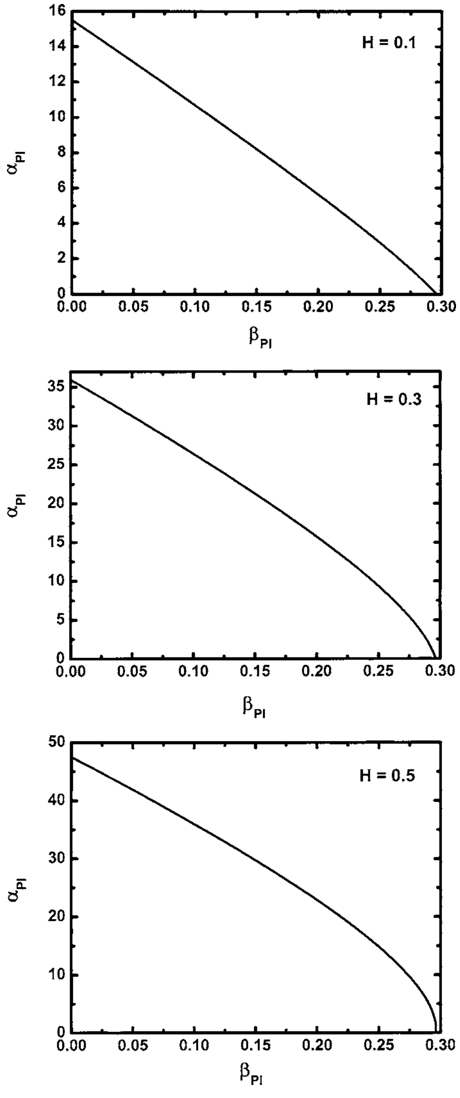

FIG. 5. Parameter α_{PI} vs β_{PI} for various roughness exponents H, $d=100$ nm, $\xi=200$ nm, and $w=10$ nm.

Equations (13) are the basic ones that will be used in our further analysis. Figure 3 shows plots of the pull-in parameter α_{PI} as a function of u_{PI} for various roughness exponents H. It is evident that the short wavelength roughness details as described by the exponent H have a significant influence on legitimate values of α_{PI} so that $\alpha_{PI}>0$ if $u_{PI}>0.66$. With decreasing exponent H or for rougher surfaces at short wavelengths ($<\xi$), the pull-in parameter α_{PI} decreases. Notably the influence of H is prominent for values $u_{PI}\sim 1$ or for plate separations comparable with the initial plate distance d. In addition, Fig. 4 shows that the allowed values of $\beta_{PI}>0$ cover a limited range of values for $0.3<u_{PI}<0.9$ depending on H. Indeed, in the case of the pull-in parameter β_{PI} the influence of the exponent H is less prominent for the range $u_{PI}>0.67$ where also $\alpha_{PI}>0$ as can be seen in Fig. 3 (see also Fig. 5). If we compare Figs 2 and 3, and Fig. 6 where the effect of the correlation length in investigated, we can infer that the roughness exponent H has a prominent influence on both pull-in parameters α_{PI} and β_{PI}.

A common plot of α_{PI} vs β_{PI} for three different exponents H is given in Fig. 5 requiring that $\beta_{PI}>0$ and $\alpha_{PI}>0$. The allowed values for β_{PI} are in the range $0<\beta_{PI}<0.3$ so that also $\alpha_{PI}>0$. The latter parameter extends to significant higher values as long as the roughness exponent H increases. Indeed, significant changes of the parameter α_{PI} occur in the range of roughness exponents $0<H\leqslant 0.5$, while for $H>0.5$ the effect of the roughness exponent starts to saturate rather fast as H approaches values close to 1 (see also Fig. 2). The largest influence of the exponent H on α_{PI} occurs for small values of $\beta_{PI}\sim 0$ or alternatively for weak electrostatic forces (or $V\ll\sqrt{kd^3/\varepsilon_0 A_r}$).

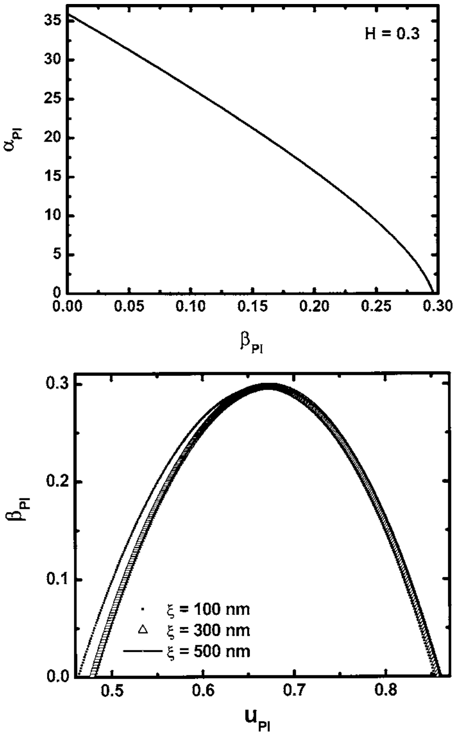

FIG. 6. Parameter α_{PI} vs u_{PI} and β_{PI} vs u_{PI} for roughness exponents $H=0.5$, $d=100$ nm, and various correlation lengths ξ, and $w=10$ nm.

V. CONCLUSIONS

In conclusion, we have investigated the influence of self-affine roughness on the pull-in parameters for switches used in MEMS/NEMS. The roughness effect was considered through its influence on the Casimir force. It was shown that the roughness exponent H has a significant influence on the Casimir force and as a result on the system pull-in parameters. Indeed, significant changes of the parameter α_{PI} that describes the ratio of the Casimir/restoring forces occur in the range of roughness exponents $0<H\leqslant 0.5$, whereas for $H\leqslant 0.5$ the effect of H saturates rather fast as the latter approaches values close to 1. In the case of the pull-in parameter β_{PI} that describes the ratio of electrostatic/restoring forces the influence of the roughness exponent H is less prominent for the range $u_{PI}>0.67$ where also we have $\alpha_{PI}>0$. The largest influence of the exponent H on α_{PI} occurs for small values of $\beta_{PI}\sim 0$ or alternatively for weak electrostatic forces so that $V\ll\sqrt{kd^3/\varepsilon_0 A_r}$.

We should point out also that the calculations with small roughness exponents ($H<0.3$) in the present calculations should be considered with caution since in this case the strong roughness limit is approached (or $\rho_{rms}\sim 1$). The latter makes the applicability of Eq. (6) for the Casimir energy questionable because higher order terms should be considered. Moreover, the effect of finite conductivity[30] should be also taken into account. These will be the topics of future works.

APPENDIX

Analytical results for the general roughness term C_r (and thus of C_r) are obtained for the roughness exponents $H=0$, 0.5, and 1:

$$C_r\big|_{H=0}=\sum_{m=1}^{2} {w_m}^2\left\{\frac{1}{a_m}(Q_c-Q_d)-\frac{1}{{a_m}^{3/2}\xi_m}[\,\tan^{-1}(u)\big|_{X_{md}}^{X_{mc}}]\right\}, \tag{A1}$$

$$C_r\big|_{H=0.5}=\sum_{m=1}^{2} {w_m}^2\left\{\frac{1}{{a_m}^{3/2}\xi_m}[\,\sinh^{-1}(u)\big|_{X_{md}}^{X_{mc}}]-\frac{1}{a_m}[Q_c{T_{mc}}^{-1/2}-Q_d{T_{md}}^{-1/2}]\right\} \tag{A2}$$

$$C_r\big|_{H=1}=\sum_{m=1}^{2} {w_m}^2\left\{\frac{1}{{a_m}^{3/2}\xi_m}[\,\tan^{-1}(u)\big|_{X_{md}}^{X_{mc}}]-\frac{1}{2a_m}[Q_c{T_{mc}}^{-1}-Q_d{T_{md}}^{-1}]\right\} \tag{A3}$$

with $L(x)|_A^B=L(B)-L(A)$, $X_{mc}=\sqrt{a_m}\xi_m Q_c$, $X_{md}=\sqrt{a_m}\xi_m Q_d$, $Q_d=2\pi/d$, $T_{mc}=1+(X_{mc})^2$, and $T_{md}=1+(X_{md})^2$.

---

*Author to whom correspondence should be addressed. Electronic address: g.palasantzas@rug.nl

[1] P. Kim and C. M. Lieber, Science **286**, 2148 (1999).

[2] S. Akita, Y. Nakayama, S. Mizooka, Y. Takano, T. Okawa, Y. Miyatake, S. Yamanaka, M. Tsuji, and T. Nosaka, Appl. Phys. Lett. **79**, 1691 (2001).

[3] P. M. Osterberg, Ph.D. thesis, Massachusetts Institute of Technology, 1995.

[4] O. Bochobza-Degani and Y. Nemirovsky, Sens. Actuators, A **97–98**, 569 (2002).

[5] O. Bochobza-Degani, E. Socher, and Y. Nemirovsky, Sens. Actuators, A **97**, 563 (2002).

[6] L. X. Zhang, J. W. Zhang, Y.-P. Zhao, and T. X. Yu, Int. J. Nonlinear Sci. Numer. Simul. **3**, 353 (2002).

[7] L. X. Zhang and Y.-P. Zhao, Microsyst. Technol. **9**, 420 (2003).

[8] L. J. Hornbeck, US Patent No. 5,061,049 (1991).

[9] J. A. Pelesko, Proc. Modeling Simulation Microsystems (MSM), 2001, p. 290.

[10] D. Bernstein, P. Guidotti, and J. A. Pelesko, Proc. Modeling Simulation Microsystems (MSM), 2000, p. 489.

[11] M. Dequesnes, S. V. Rotkin, and N. R. Aluru, Nanotechnology **13**, 120 (2002).

[12] S. V. Rotkin, in *Microfabricated Systems and MEMS VI*, Electrochemical Society Proceedings, Philadelphia, PA, 2002, edited by P. Hesketh, S. S. Ang, J. L. Davidson, H. G. Hughes, and D. Misra, PV 2002-6, p. 90, http://www.electrochem.org/publications/pv/published/2002.htm

[13] W. H. Lin and Y.-P. Zhao, Chin. Phys. Lett. **20**, 2070 (2003).

[14] R. Seydel, *Practical Bifurcation and Stability Analysis: From Equilibrium to Chaos*, Interdisciplinary Applied Mathematics Vol. 5, 2nd ed. (Springer, New York, 1994).

[15] W. H. Lin and Y.-P. Zhao, Chaos, Solitons Fractals **23**, 1777 (2005).

[16] H. B. G. Casimir, Proc. K. Ned. Akad. Wet. **51**, 793 (1948).

[17] J. N. Israelachvili, *Intermolecular and Surface Forces* (Academic, London, 1992).

[18] K. A. Milton, Phys. Rev. D **22**, 1441 (1980); **22**, 1444 (1980).

[19] I. Brevik and H. Kolbenstvedt, Nuovo Cimento Soc. Ital. Fis., B **82B**, 71 (1984).

[20] G. Plunien, B. Muller, and W. Greiner, Phys. Rep. **134**, 87 (1986).

[21] V. M. Mostepanenko and N. N. Trunov, *The Casimir Effect and its Applications* (Clarendon, Oxford, 1997).

[22] E. Elizalde and A. Romeo, Am. J. Phys. **59**, 711 (1991).

[23] P. W. Milonni, *The Quantum Vacuum* (Academic, San Diego, 1994).

[24] M. Kardar and R. Golestanian, Rev. Mod. Phys. **71**, 1233 (1999); H. Li and M. Kardar, Phys. Rev. Lett. **67**, 3275 (1991); H. Li and M. Kardar, Phys. Rev. A **46**, 6490 (1992).

[25] P. Meakin, Phys. Rep. **235**, 1991 (1994); J. Krim and G. Palasantzas, Int. J. Mod. Phys. B **9**, 599 (1995).

[26] C. Genet, A. Lambrecht, P. Maia Net, and S. Reynaud, Europhys. Lett. **62**, 484 (2003).

[27] T. Emig, A. Hanke, R. Golestanian, and M. Kardar, Phys. Rev. Lett. **87**, 260402 (2001). Equations (5) and (6) in this work yield the expressions for TE and TM modes.

[28] G. Palasantzas, Phys. Rev. B **48**, 14472 (1993); **49**, 5785 (1994).

[29] S. K. Sinha, E. B. Sirota, S. Garoff, and H. B. Stanley, Phys. Rev. B **38**, 2297 (1988); H. N. Yang and T. M. Lu, Phys. Rev. E **51**, 2479 (1995); Y. P. Zhao, G. C. Wang, and T. M. Lu, Phys. Rev. B **55**, 13938 (1997).

[30] P. A. Maia Neto, A. Lambrecht, and S. Reynaud, Europhys. Lett. **69**, 924 (2005).

[31] B. N. J. Persson and E. Tosatti, J. Chem. Phys. **115**, 3840 (2001).

[32] G. Palasantzas, Phys. Rev. E **56**, 1254 (1997).